Deep-Sea Research II 55 (2008) 1594–1604

Contents lists available at ScienceDirect

Deep-Sea Research II

journal homepage: www.elsevier.com/locate/dsr2

Primary, new and export production in the NW Pacific subarctic gyre during the vertigo K2 experiments

M. Elskens [a,*], N. Brion [a], K. Buesseler [b], B.A.S. Van Mooy [b], P. Boyd [c], F. Dehairs [a], N. Savoye [d], W. Baeyens [a]

[a] Department of Analytical and Environmental Chemistry, Vrije Universiteit Brussel, Pleinlaan 2, B-1050 Brussels, Belgium
[b] Department of Marine Chemistry and Geochemistry, Woods Hole Oceanographic Institution, MA 02543, USA
[c] Department of Chemistry, NIWA Centre for Physical and Chemical Oceanography, University of Otago, Dunedin, New Zealand
[d] Observatoire Aquitain des Sciences de l'Univers, UMR EPOC, Université Bordeaux 1– CNRS, Station Marine d'Arcachon, 2 rue du Pr. Jolyet, Arcachon, France

ARTICLE INFO

Article history:

Accepted 13 April 2008
Available online 7 May 2008

Keywords:
f ratio
New production
e ratio
Export production
Carbon and nitrogen budget

ABSTRACT

This paper presents results on tracer experiments using ^{13}C and ^{15}N to estimate uptake rates of dissolved inorganic carbon (DIC) and nitrogen (DIN). Experiments were carried out at station K2 (47°N, 161°E) in the NW Pacific subarctic gyre during July–August 2005. Our goal was to investigate relationships between new and export production. New production was inferred from the tracer experiments using the *f* ratio concept (0–50 m); while export production was assessed with neutrally buoyant sediment traps (NBSTs) and the *e* ratio concept (at 150 m). During trap deployments, K2 was characterized both by changes in primary production (523–404 mg C m^{-2} d^{-1}), new production (119–67 mg C m^{-2} d^{-1}), export production (68–24 mg C m^{-2} d^{-1}) and phytoplankton composition (high to low proportion of diatoms). The data indicate that 17–23% of primary production is exportable to deeper layers (*f* ratio) but only 6–13% collected as a sinking particle flux at 150 m (*e* ratio). Accordingly, >80% of the carbon fixed by phytoplankton would be mineralized in the upper 50 m (1–*f*), while <11% would be within 50–150 m (*f*–*e*). DIN uptake flux amounted to 0.5 mM m^{-2} h^{-1}, which was equivalent to about 95% particulate nitrogen (PN) remineralized and/or grazed within the upper 150 m. Most of the shallow PN remineralization occurred just above the depth of the deep chlorophyll maximum (DCM), where a net ammonium production was measured. Below the DCM, while nitrate uptake rates became negligible because of light limitation, ammonium uptake did continue to be significant. The uptake of ammonium by heterotrophic bacteria was estimated to be 14–17% of the DIN assimilation. Less clear are the consequences of this uptake on the phytoplankton community and biogeochemical processes, e.g. new production. It was suggested that competition for ammonium could select for small cells and may force large diatoms to use nitrate. This implies that under Fe stress as observed here, ammonium uptake is preferred and new production progressively suppressed despite the surplus of nitrate.

1. Introduction

Early approaches to investigate the efficiency of particle export between the surface and subsurface ocean were restricted to surface waters and deep-ocean processes (Pace et al., 1987) leading to the introduction of the new production paradigm. "The sinking flux of particulate organic carbon in the deep ocean is quantitatively equivalent to the organic matter that can be exported from the total production in the euphotic zone without the production system running down" (Eppley and Peterson, 1979). This concept is one of the cornerstones of biogeochemistry since it constrains both the sustainable exploitation of marine resources and the role of the oceans in the regulation of excess anthropogenic CO_2 accumulation in the atmosphere (Longhurst and Harrison, 1989). New production is merely defined as the portion of primary production driven by externally supplied nutrients (where external refers to sources outside the euphotic zone including upwelling, atmospheric deposition and nitrogen fixation). The resulting ratio of new to total primary production is called the *f* ratio. The determination of ^{15}N nitrogen uptake enables the separation of new from regenerated production—i.e. of primary production sustained by nitrate and N_2 from that sustained by regenerated N-nutrients such as ammonium and amino acids (Dugdale and Goering, 1967). Assuming a steady state nutrient budget for the upper ocean and an absence of nitrate regeneration in the euphotic zone, Eppley and Peterson (1979) have linked new production to export production via the use of *f* ratio. Although the concept of *f* ratio is simple, its estimation can

* Corresponding author.
E-mail address: melskens@vub.ac.be (M. Elskens).

0967-0645/$ - see front matter © 2008 Elsevier Ltd. All rights reserved.
doi:10.1016/j.dsr2.2008.04.013

be rather complicated, and has been controversial (Eppley, 1989; Platt et al., 1992; Bronk et al., 1994; Yool et al., 2007). For example, the production of dissolved organic matter by natural phytoplankton assemblages, its downward advection and diffusion may bias estimates of new production and its relation with the export of organic particles from the trophogenic zone. However, no other current techniques can yield comparable data on nitrogen flux, and new production should better be regarded as "exportable production" rather than "export production" (see Sambrotto and Mace, 2000; Reuter et al., 2007). Alternatives to ^{15}N new production assessment have since been proposed, e.g., sediment traps at the base of the photic zone and the thorium–uranium disequilibria, but these methods have their own drawbacks (Buesseler et al., 2006, 2007b). The VERtical Transport in the Global Ocean (VERTIGO) research project overcame many of the issues of trap collection biases in mesopelagic waters by using Neutrally Buoyant Sediment Traps (NBSTs). These traps are designed to sink to predetermined depths via accurate ballasting and to drift along with the prevailing current, thereby avoiding problems related with flow perturbation typical for bottom and surface tethered traps (Buesseler et al., 2007b and references therein).

The specific objective of this paper is to investigate relationships between new (potential carbon/nitrogen export flux from the photic zone) and export productions (sinking flux of particulate organic carbon/nitrogen POC/PN collected at the base of the photic zone). New production was inferred from ^{15}N tracer experiments using the traditional definition of f ratio; while export production was assessed with NBSTs and the e ratio concept that is the measured 150 m POC flux to primary production ratio. Our ultimate goal is to determine how much of the carbon and nitrogen assimilated by phytoplankton is mineralized in the trophogenic zone, hence providing an estimate of the potential supply of organic matter to the twilight zone, a dim region 100–1000 m below the surface, where the attenuation in particle flux with depth is particularly pronounced.

2. Methods

2.1. Site description

K2 (47°N, 161°E) is a mesotrophic site in the NW Pacific subarctic gyre, characterized by high surface nutrients, including silica, and a clear dominance of the phytoplankton community by diatoms (Honda, 2003; Honda et al., 2006; Buesseler et al., 2008). There is significant annual variability in surface chlorophyll, ranging from 0.1 to 0.8 mg m^{-3} and possibly higher with substantial small-scale variability (Fig. 2 in Buesseler et al., 2008). There is also apparent and variable drawdown of macronutrients as the season progresses (Table 1 in Buesseler et al., 2008).

Table 1
Uncertainty/variability dichotomy in assessing uptake (U) and regeneration (R) rates of dissolved inorganic carbon and nitrogen

Substrate	Tracer addition %	Rate	Relative uncertainty %	Relative variability %	Accuracy
$^{15}NH_4Cl$	2–14	UNH_4	7.7	14.4	$<\chi^2_{95\%}$
		RNH_4	22.7	22.4	$<\chi^2_{95\%}$
$K^{15}NO_3$	1–2	UNO_3	17.7	34.6	$<\chi^2_{95\%}$
		RNO_3	–	–	<MDL
$^{15}N_2$	7–10	UN_2	–	–	<MDL
$Na_2{}^{13}CO_3$	8–11	UC	5	21	$<\chi^2_{95\%}$

Uncertainty represents the random error propagations through rate calculations, while variability covers changing environmental conditions and sampling. Accuracy refers to the probability of the residual cost function value. It is acceptable when $<\chi^2_{95\%}$ (Section 2.8). MDL stands for method or model detection limit.

As determined from SeaWIFS images (Honda and Watanabe, 2007), we arrived at K2 in 2005 about 20–30 days after the seasonal maximum in phytoplankton biomass, and prior to a slightly smaller autumn bloom. The 150 m POC flux data show a significant drop off during the cruise reflecting the termination of a diatom bloom, and is echoed in the record from deep moored traps (Buesseler et al., 2007a). As a result biogenic silica appears to be the major constituent of trapped material with 80% by weight being opal (Buesseler et al., 2007a; Lamborg et al., 2008).

2.2. The tracer experiments

The design of experiments for the simultaneous determination of inorganic carbon and nitrogen uptake rates involved the addition of enriched ^{15}N (as NH_4Cl, KNO_3 and N_2) and ^{13}C substrates (as Na_2CO_3) to water samples, and after some period of incubation measuring the ^{15}N and ^{13}C incorporated into particulate material. Seawater was sampled using Niskin bottles at four depths (~10, 20, 40, 50 m). The changes in substrate concentrations and abundances of the particulate pools were measured just after spiking, and after 3 incubation times (~2, 4, 6 h). The kinetic experiments were conducted on deck in a simulated *in situ* light (4 levels from 100% to 1% of the surface irradiance tuned with appropriate neutral density screens) and temperature controlled incubator. The sampling was repeated 8 times during trap deployments D1 (30/07–07/08/2005; CTD biocasts 18, 23, 31, 39) and D2 (10/08–18/08/2005; CTD biocasts 62, 66, 76, 84) providing a total of about 500 tracer experiments. Full CTD and bottle data are available on line at http://ocb.whoi.edu/vertigo.html. Maps of drifting sediment trap trajectories, deployment and retrieval sites for NBSTs and locations of biocast CTD stations are shown in Fig. 6 of Buesseler et al. (2008). In the experimental set up the initial abundance of the substrate pools was calculated with an isotope dilution law (Harrison, 1983). Tracer additions were variable ranging from 1% to 14% of the ambient substrate pools as shown in Table 1. Dark bottles incubations for carbon and nitrogen uptakes were also performed with water samples collected at 70 m.

2.3. Analytical procedures

Ammonium concentrations were determined manually aboard ship with the Berthelot reaction following Koroleff (1976). Detection limit was around 0.05 μmol L^{-1}. Water samples for the determination of nitrate and nitrite were filtered through cellulose membranes (Millipore type Millex-HA, 0.45 μM) stored in polyethylene bottles and frozen until analysis in the home laboratory with a Technicon Auto-Analyser II. The procedure involved the reduction of nitrate to nitrite on a Cu–Cd column, and the subsequent determination of nitrite with the Griess reaction following Hansen and Grasshof (1983). Detection limit was around 0.1 μmol L^{-1}. Particulate nitrogen and carbon were collected by filtration (1 L) on combusted GF/F glass-fibre (Whatman) after each time step. The filters were dried at 50 °C for 8 h and pretreated with HCl acid vapor to remove carbonates prior analysis of PN and POC concentration along with their ^{15}N and ^{13}C abundances. In all cases, the abundances and concentration of the particulate matter were measured using an elemental analyzer (Carlo-Erba C/N analyzer) coupled via a conflo-interface to an isotope ratio mass spectrometer Finnigan Delta-Plus XL (Nieuwenhuize et al., 1994). Standard deviations on concentrations and isotopic ratios are based on long-term within-laboratory reproducibility estimates. For nitrate and ammonium determinations, relative standard deviation (RSD) are variable ranging from 2% to 15% (D'Elia, 1983 and references therein). For particulate materials, Nieuwenhuize et al. (1994) reported RSD values close to

4%. For isotope analysis, results obtained during collaborative studies on enriched ^{15}N (IAEA-311) and ^{13}C (IAEA-309B) reference materials indicated RSD less than 0.5%. However, actual precision may be lower than the quoted value, particularly with enriched sample that has been processed through all steps of the incubation protocol. In our laboratory RSD on ^{13}C and ^{15}N enrichment are less than 5% for replicate measurements (Elskens et al., 2005).

2.4. Bacterial production and carbon demand

Bacterial production (BP) was determined using [methyl-^{3}H]-thymidine (TdR) incorporation incubations conducted at atmospheric pressure and *in situ* temperatures (Fuhrman and Azam, 1982). Triplicate, acid-washed 30 mL polycarbonate bottles were filled with seawater from each depth and spiked with 20 nmol L^{-1} of TdR. Replicate incubations were poisoned with 3% formaldehyde prior to addition of TdR. All bottles were incubated for 24 h. TdR incorporation rates were determined following trichloroacetic acid precipitation and filtration as described by Carlson et al. (1996). BP was calculated from TdR incorporation rates using TdR conversion factors of $1–2 \times 10^{18}$ cells mol^{-1} and a carbon conversion factor of 15 fg C $cell^{-1}$; these values approximate the median of those published for bacterial communities in surface waters (Ducklow, 2000 and references therein). Bacterial carbon demand (BCD) was calculated using a bacterial growth efficiency (BGE) ranged between 0.10 and 0.15, which was also derived from published values for surface bacterial communities (del Giorgio and Cole, 2000).

2.5. Neutrally buoyant sediment trap (NBST)

NBST trap was deployed at 150 m for primary flux measurement. Briefly, NBST is a free vehicle that sinks to a preprogrammed sampling depth for 3–5 days deployments and drifts with local currents, thus minimizing possible hydrodynamic biases (Buesseler et al., 2007b and references therein). Detailed descriptions of the NBST methodology along with protocols for blanks, swimmer removal, sample preservation and sampling handling and analytical methods are presented in Lamborg et al. (2008).

2.6. Calculation of nitrogen and carbon uptake

The most widespread ^{15}N and ^{13}C model is derived from the isotopic and mass balances in the particulate fraction providing the commonly used formula Eq. (1) for nitrogen and carbon uptakes (Dugdale and Goering, 1967; Legendre and Gosselin, 1996):

$$\frac{ÆP(t) \cdot P(t)}{ÆS(i)} = U(t) \cdot t \quad (1)$$

where $ÆP(t)$ stands for the ^{15}N or ^{13}C atom% excess in the particulate matter at time t, $ÆS(i)$ is the initial ^{15}N or ^{13}C atom% excess of the substrate pool, $P(t)$ the POC or PN concentration at time t and $U(t)$ the nitrogen or carbon uptake rate.

Plotting the left term of Eq. (1) as a function of time does not necessarily result in a straight line with a near zero intercept and a constant slope $U(t)$ (Fig. 1). The departure to linearity (the fall-off in the reaction rate) is due to isotope dilution and tracer release during incubation (Elskens et al., 2005 and references therein). Therefore, the choice between straight line and curvilinear regression methods is made using a Mandel's fitting test (Mandel, 1964). In these regressions, the initial rate, U at $t = 0$ is given by the first-order coefficient and yields an estimate of gross uptake rate with unit $\mu M\,h^{-1}$. This procedure facilitates data treatment and model analysis because it does not require any assumption about rate law expression (see Section 2.7). Overall the precision on uptake estimates averaged 5–18% (Table 1). From Eq. (1) one also estimate a detection or decision limit for the uptake rate according to the IUPAC recommendations (Currie, 1995):

$$DL = 3 \cdot \sqrt{2} sd_{\alpha n} \quad (2)$$

where $sd_{\alpha n}$ is the standard deviation of the natural background value.

DL is defined as the critical level or decision limit above which an observed signal $ÆP(t)$ may be reliably recognized as detected. It amounts to 0.017 and 0.008 atom% for ^{13}C and ^{15}N, respectively. For that reason all $ÆP(t)$ below DL will provide uptake rates, which are not significantly different from 0 (Table 1).

Daily primary production was obtained by multiplying the hourly ^{13}C data (see above) by the day light period. These values assumed to represent the net primary production (NPP) were not corrected for dark uptake since the latter was below detection. The total euphotic zone NPP (mg C $m^{-2}\,d^{-1}$) was assessed using the trapezoid rule and integrated to ~55 m, the depth of the 0.1% light penetration. A comparison between NNP data obtained with ^{13}C and ^{14}C (Boyd et al., this issue) techniques are discussed below in the text. For nitrogen daily values were not calculated. Depending on length of incubation, different cellular metabolic processes may be measured (Glibert and Capone, 1993). Therefore,

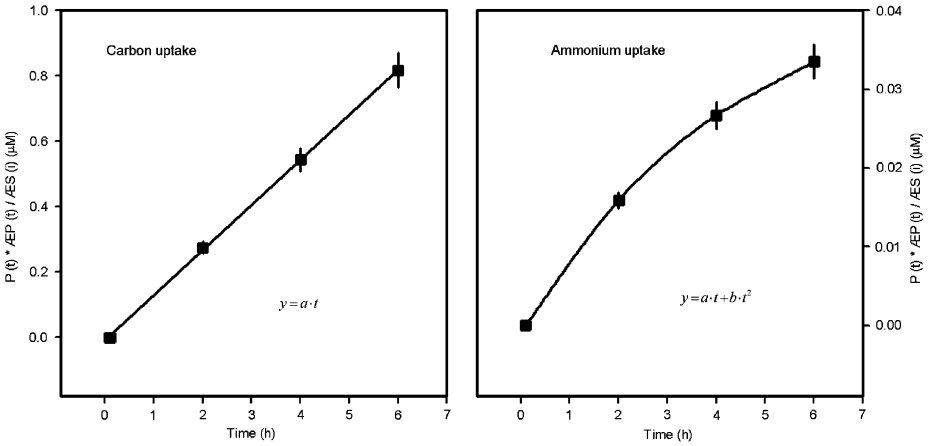

Fig. 1. Examples of data, linear *vs.* curvilinear fits and parameter estimates for carbon and nitrogen uptake rates Eq. (1). The error bars represent the uncertainty on rate calculations (propagation of random errors, Section 2.8). The choice between the linear and quadratic model is made using a Mandel's fitting test (Mandel, 1964). The initial rate U at $t = 0$ is given by a, which provides an estimate of gross uptake rate with unit $\mu M\,h^{-1}$.

gross uptake as determined here is probably less ambiguous to consider (Elskens et al., 2005). The total euphotic zone nitrogen based production UDIN ($mM\,m^{-2}\,h^{-1}$) was integrated as described above. We estimate the bacterial uptake of inorganic nitrogen using the formula introduced by Kirchman (1994):

$$\%\text{N-uptake} = 1.4 \cdot \frac{BP}{NPP} \quad (3)$$

where BP and PP are the bacterial and net primary production, respectively, and 1.4 a correction factor taking into account differences in C/N ratios between phytoplankton and bacteria. Since nitrate uptake by heterotrophic bacteria is usually low, it can be safely ignored as a first approximation (Kirchman, 1994). Eq. (3) gives thus an estimate of the bacterial ammonium uptake.

2.7. Calculation of nitrogen regeneration

Compartmental model analysis was used to assess nitrogen regeneration (ammonification and nitrification rates). The three compartment open model depicted in Fig. 2 is similar to the generic models described in Elskens et al. (2002, 2005), and assumes that exchange between compartments is governed by first-order differential equations with constant coefficients of the general type:

$$\frac{dX_i}{dt} = \sum_{j \neq i}^{n} k_j X_j - \sum_{i \neq j}^{n} k_i X_i \quad (4)$$

where X are the nitrogen isotopes (^{15}N or ^{14}N) in compartment i at time t, k is the rate constant for transport between compartments (in reciprocal time units).

With uptake rates being determined, the remaining parameters to be optimized are R_A, kr_N and kl_P (Fig. 2). The mass balance differential equations (Eq. (4)) are solved numerically (Elskens et al., 1988) and optimization achieved using weighted least-squares techniques. Statistical inferences about parameter values and model outcomes are performed as described in Elskens et al. (2005, 2007) (Section 2.8).

2.8. Quality control analysis

Optimal tracer addition, considered as $<10\%$ of the ambient substrate concentration (Dugdale and Goering, 1967) was nearly always achieved (Table 1), and thus one can consider that *in situ* rates of uptake have been addressed in this study (Glibert and Capone, 1993). Uncertainty on uptake and regeneration represents the propagation of random errors through rate calculations. It can be seen from Eq. (5) that the relative standard uncertainty (RSU) on uptake is not much larger than the largest relative standard deviation used to calculate it:

$$RSU_{uptake} = \frac{100}{t} \cdot \sqrt{\left(\frac{\sigma_{ÆP}}{ÆP}\right)^2 + \left(\frac{\sigma_{ÆD}}{ÆD}\right)^2 + \left(\frac{\sigma_{PN}}{PN}\right)^2} \quad (5)$$

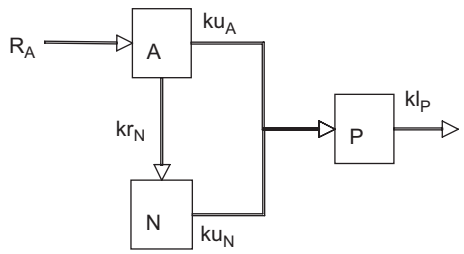

Fig. 2. Three compartments open model describing exchange reactions between ammonium (A), nitrate (N) and particulate organic nitrogen (P). k: rate constants (t^{-1}), r: regeneration, l: loss, u: uptake, R_A: ammonium regeneration rate ($\mu M\,t^{-1}$).

As a corollary to this, when a tracer addition is much less than 10% of ambient is made such as for nitrate, the atom% excess in the particulate fraction ÆP is very small, its relative standard deviation increases and RSU_{uptake} dramatically rises (Table 1). Despite optimal tracer additions for N_2, ÆP remained below DL Eq. (2) and thus the rates were insignificant ($<$Method Detection Limit or MDL). This probably results from the fact that N_2 fixation (i) is not energetically favorable when ammonium is available, and (ii) requires nearly 100 times more iron than any other means of nitrogen assimilation (Falkowski, 1997; Orcutt et al., 2001) while K2 is apparently iron limited (Boyd et al., this issue). Finally, the best conditions were encountered during the carbon and ammonium assimilation experiments with RSU values of 5–8% (Table 1). In contrast herewith, solutions for regeneration rates cannot be expressed explicitly, and are sought with an iterative method (Marquardt–Levenberg algorithm). The standard error on the regression coefficient was assessed using variance–covariance matrix as described in de Brauwere et al. (2005a). A t statistic (t is the ratio of the regression coefficient to its standard error) is computed to test whether the estimated parameter is significant. For nitrate the t-test indicated that the rate constant kr_N could be removed from the model regression without affecting the goodness of fit meaning that RNO_3 rates were insignificant ($<$MDL, Table 1). For ammonium, the RSU on RNH_4 was in the order of 23%. The accuracy of the model outcome (goodness of fit or agreement between the observations and the model counterparts) is tested with a χ^2 statistic. When the sum of the weighted least squares residuals falls within the 95% confidence limit of a χ^2 distribution, the model results are regarded as being satisfactory (de Brauwere et al., 2005b). We make a distinction between variability and uncertainty. This dichotomy has become conventional in environmental assessments (Suter, 2007). Variability is an intrinsic property of the system and covers changing environmental conditions and sampling heterogeneity. It ranges from 14% to 35% (Table 1).

3. Results and discussion

3.1. Surface euphotic zone

The surface mixed layer (ML) was estimated by visual inspection of CTD profiles associated with trap deployments. Generally a well-defined thermocline was present, showing a shallow 25 m summer time ML above the temperature minimum of $<2\,^{\circ}C$ near 100 m (Fig. 3). The limit of the euphotic zone, defined as equal to the depth of 0.1% light penetration was estimated around 55 m, and coincided roughly with the depth of the deep chlorophyll maximum (DCM). Nitrate concentrations remained high, greater than 13 μM in the upper ML, increasing up to ~30 μM near 100 m. Ammonium concentration peaked at $>1.5\,\mu M$ just above the DCM, and was shallower than the nitrite maximum observed just below the DCM (Fig. 3).

While the nitrate and nitrite stocks did not change significantly between trap deployments (D1 and D2), a build-up of ammonium was found in the first 10 days of sampling with a net production rate of 3.2 (SE = 0.4) $mmol\,m^{-2}\,d^{-1}$ (Fig. 4). Suspended organic carbon and nitrogen followed exponential type decay *vs.* depth in the euphotic zone with C/N ratios closed to Redfield. Both particulate stocks decreased almost linearly throughout sampling with net consumption rates of 0.95 (SE = 0.15) $mmol\,m^{-2}\,d^{-1}$ for N and 6.4 (SE = 1.5) $mmol\,m^{-2}\,d^{-1}$ for C (Fig. 5). These rates most likely reflect sinking and grazing losses. This overall decrease in phytoplankton biomass indicated the end of a regional diatom bloom that had peaked several weeks prior to our arrival, and is supported by deep trap fluxes of biogenic silica and POC (Honda, unpublished data).

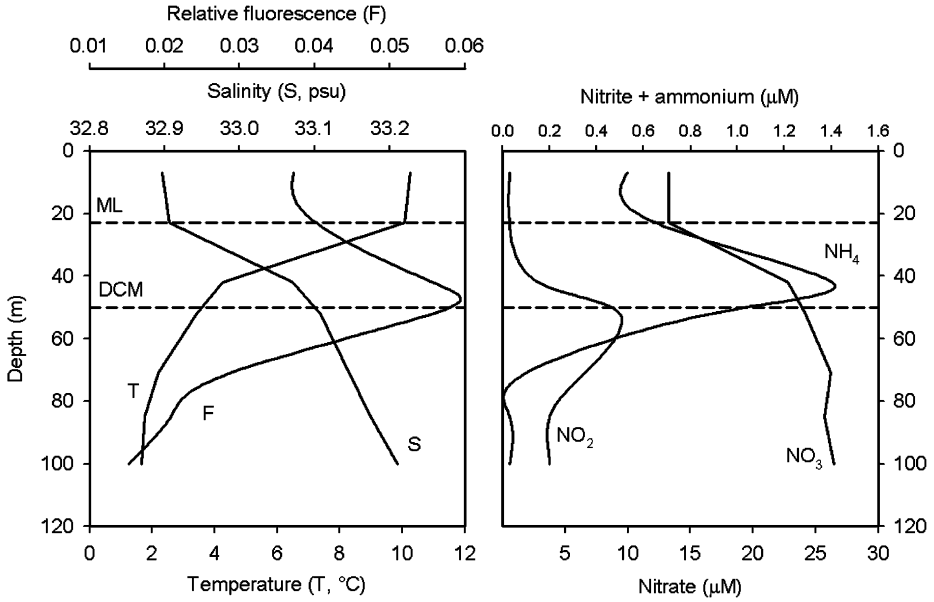

Fig. 3. Typical vertical profiles of temperature, salinity, fluorescence and DIN concentrations at K2. Full CTD and bottle data are available on line at http://ocb.whoi.edu/vertigo.html.

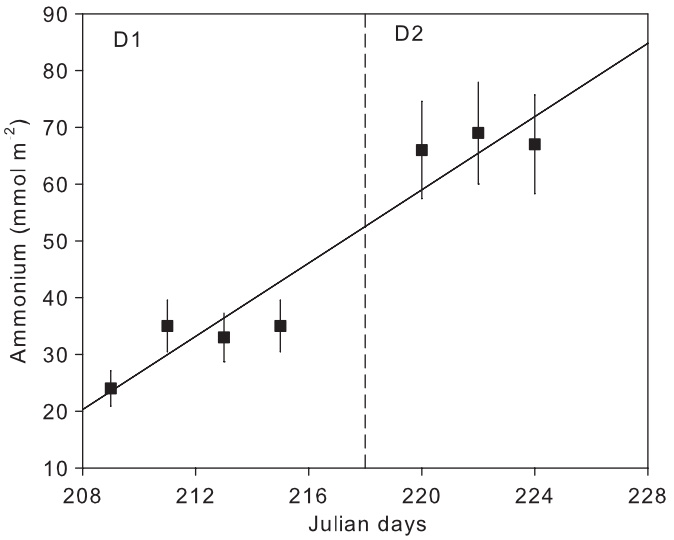

Fig. 4. Depth-integrated ammonium stocks (0–50 m) during the trap deployments (D1 and D2). The errors bars represent the within-laboratory reproducibility (Section 2.3). The slope $dNH_4/dt = 3.2$ (SE = 0.4, $p<0.001$) mmol m^{-2} d^{-1}. SE: standard error. The p value is the probability that the slope does not differ from 0.

3.2. Carbon and nitrogen based production

We determined that the N_2 fixation rates were insignificant and thus the principal sources of inorganic nitrogen for phytoplankton nutrition are ammonium and nitrate (Table 1; Fig. 6). In the vicinity of the DCM, while nitrate uptake rates became negligible because of light limitation, ammonium uptake did continue to be significant. Since heterotrophic bacteria can account for a large fraction of total ammonium assimilation (Kirchman, 1994), we estimated this contribution using Eq. (3). The percentage attributable to bacteria amounted to 14–17%, which roughly corresponds to the lower quartile range of the values reported by Kirchman (1994) for marine systems. It reflects an averaged bacterial to primary production ratio of ~11% (Table 2). This is consistent with other synthesized data in the subarctic Pacific, where bacterial production was found to represent 5–15% of the local primary production (Kirchman et al., 1993). It was also suggested that bacterial ammonium uptake in the subarctic Pacific could be limited by the supply of organic carbon (Kirchman et al., 1990). Euphotic zone depth-integrated nitrogen production decreased from 0.53 (SE = 0.02) during D1–0.44 (SE = 0.04) mmol m^{-2} h^{-1} during D2. While ammonium uptake did not change significantly, fluctuating randomly around 0.39 (SE = 0.02) mmol m^{-2} h^{-1}, nitrate uptake decreased regularly from 0.15 to 0.09 mmol m^{-2} h^{-1} during D1 to reach a background level of 0.07 (SE = 0.01) mmol m^{-2} h^{-1} in D2, as the diatom bloom ended (Fig. 7). It follows that the f ratio (the ratio of NO_3 based production divided by the total inorganic N production), decreased from 28% to 19% during D1 reaching an average value of 17% during D2. It is likely that these f values are maximum estimates since regenerated production on other nitrogenous substrates such as amino acids and urea were not considered in this study. It is less clear how the uptake of ammonium by heterotrophic bacteria may affect the f ratio, but competition for ammonium could select for small cells and may force large phytoplankton to use nitrate (Kirchman et al., 1990). Specific nitrate uptake rates ranged between 0.010 and 0.026 d^{-1}, which are typical values reported in HNLC waters (Dugdale and Wilkerson, 1992). It should be noted, however, that these rates are not enough to overcome biomass losses by sinking and predation.

Net primary production (NPP) was measured either by ^{13}C or ^{14}C techniques (Boyd et al., this issue), both providing essentially comparable results (paired t-test, $p = 0.324$; see Fig. 8). New production rates (“exportable production”) were then calculated as the product f ratio x NPP. During the trap deployments, K2 was characterized by a sudden decrease in primary production (523–404 mg C m^{-2} d^{-1} on an average basis) and a downward trend in new production (164–67 mg C m^{-2} d^{-1}). Synthesized data for the western subarctic Pacific (Imaii et al., 2002; Wong et al., 2002; Kawakami and Honda, 2007) indicated that primary productivity had a distinct seasonal variation with a 10-fold range during winter–spring (50–550 mg C m^{-2} d^{-1}) and that the yearly averaged new production as estimated from the seasonal drawdown of nitrate ranged from 125 to 230 mg C m^{-2} d^{-1}. These results suggest that we just missed the productivity peak for both

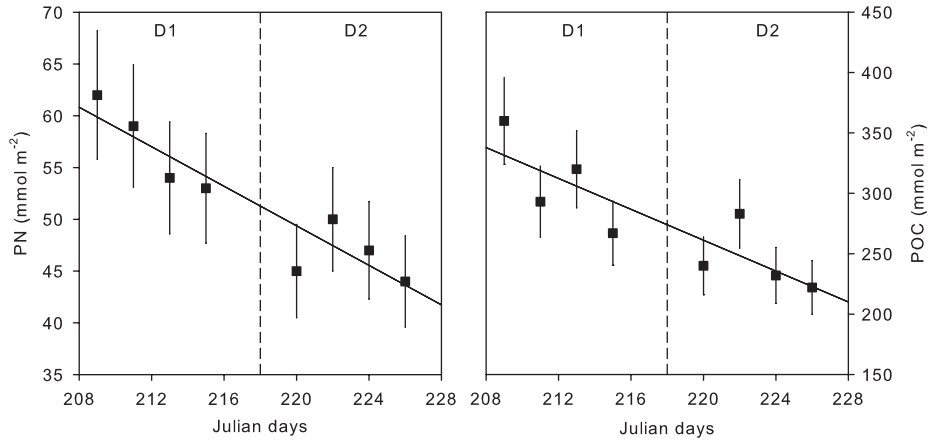

Fig. 5. Depth-integrated POC and PN stocks (0–50 m) during the trap deployments (D1 and D2). The errors bars represent the within-laboratory reproducibility (Section 2.3). Slopes $dPN/dt = -0.95$ (SE = 0.15, $p < 0.001$) and $dPOC/dt = -6.4$ (SE = 1.5, $p = 0.006$) mmol m^{-2} d^{-1}. SE: standard error. The p value is the probability that the slope does not differ from 0.

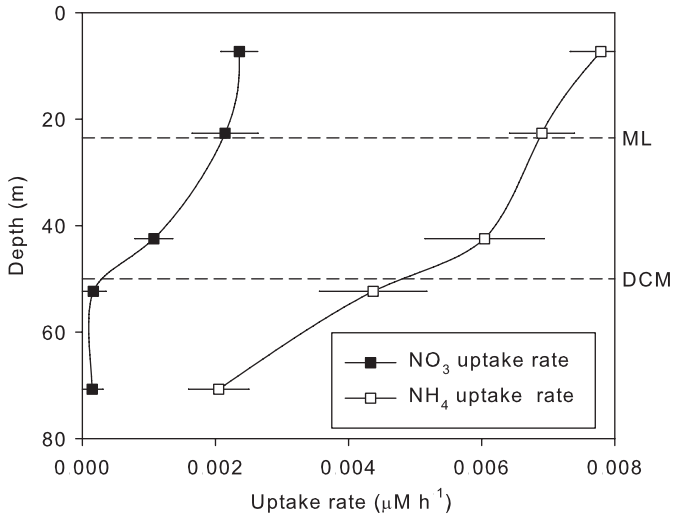

Fig. 6. Averaged profiles ($n = 8$) of DIN uptake at K2. The error bars represent the sampling variability and are expressed as standard error of the mean.

NPP and NP in July 2005. Fig. 9 shows the relationships between the measured carbon and inorganic nitrogen assimilation rates in the euphotic zone. Spearman 's rank order correlation coefficient was 0.86 ($p < 0.001$) suggesting that 74% of the variation in either variable is explained by its correlation with the other. The slope of the fitted line (regression coefficient $\pm$SE) is

$$UC = (7.6 \pm 1.0)UDIN \quad (6)$$

Photosynthesis was, however, better correlated with ammonium assimilation (Spearman $R = 0.794$, $p < 0.001$) than with nitrate (Spearman $R = 0.716$, $p < 0.001$). Multiple regression analysis indicated, moreover, that slopes of the photosynthetic rate *versus* either ammonium or nitrate assimilation rates were different:

$$UC = (6.5 \pm 1.9)UNH_4 + (9.8 \pm 3.4)UNO_3 \quad (7)$$

Possible explanations for the slope difference are as follows:

(i). Small size phytoplankton cells used ammonium preferentially over nitrate in a regenerated production loop (Harrison and Wood, 1988) and with C/N uptake ratio close to Redfield. For instance, size fractionated ^{14}C uptake experiments indicated that 0.2–2 μm phytoplankton cells represented from 50% to 59% of the total production during trap deployments (Boyd et al., this issue) and ~60% of the variation in either UC and UNH_4 are explained by their correlation. At K2, the picoplankton community was dominated by *Synechococccus*, picoeukaryotes and heterotrophic bacteria (Zhang et al., 2008, this issue).

(ii). The decline in the bloom of large diatoms exhibited progressive uncoupling between C/N uptake ratios while running mainly on new production and its nitrate source. It was shown that the >20 μm contribution to primary production decreased from 30% to 19% between D1 and D2, respectively (Boyd et al., this issue) in parallel with the decreasing f ratio (28–17%). During this period, a decrease of fucoxanthin concentration from 100 to 40 ng L^{-1} was also noted; the loss of diatoms corresponding to a relatively greater abundance of other chromatophytes with a small unchanging fraction of cyanobacteria (Buesseler et al., this issue). It was suggested that the end of the diatom bloom was caused by light and/or iron limitation. Silic acid concentrations remained high, greater than 8 μM in the upper ML increasing up to 55 μM near 100 m. Moreover values of the photosynthetic competence (Fv/Fm) are consistent with an algal iron stress (Boyd et al., 2008, this issue). If so competition for ammonium induced by heterotrophic bacteria may affect the phytoplankton community structure because the iron demand of phytoplankton cells is higher when growing on nitrate compared to ammonium as N source (Maldonato and Price, 1996). This implies that in low Fe waters ammonium uptake is preferred and new production progressively suppressed despite the surplus of nitrate.

3.3. Nitrogen regeneration

The regeneration of ammonium and nitrate was assessed using results of the ^{15}N tracer experiments and compartmental modelling (Section 2.7). The slight variations of nitrate concentration during the incubation did not allow the nitrification rate to be quantified (Table 1). The ammonium production was compared to nitrogen mineralization as estimated from bacterial production measurements (Table 2). Although these experiments were not performed each time on the same cast, they compared fairly with averaged bacterial remineralisation less than ammonium regeneration (Fig. 10). These differences are largely due to the fact that ammonium production involves both ammonification

Table 2
Carbon budget at K2

Depth (m)	Symbol	Carbon flux rate (mg C m^{-2} d^{-1})	D1 31/07–06/08/05		D2 11/08–16/08/05
0–50	NPP	Net primary production	523 ± 58		403 ± 14
	BP	Bacterial production	51 ± 2		49 ± 8
	RP = (1–*f*) NPP	Regenerated production	404 ± 42		336 ± 17
	NP = *f*. NPP	New production	119 ± 21		67 ± 12
	dPOC/d*t*	Rate of POC change (Fig. 5B)		−77 ± 12	
	HCD	Available C for heterotrophic community Eq. (8)	481 ± 62		414 ± 19
	BCD	Bacterial carbon demand	343 ± 13		328 ± 51
	1–*f*	% POC remineralization	77%		83%
50–150	NP	Exportable C flux	119 ± 21		67 ± 12
	BP	Bacterial production	9 ± 3		10 ± 3
	dPOC/d*t*	Rate of POC change		~0	
	HCD	Available C for heterotrophic community Eq. (8)	51 ± 21		45 ± 12
	BCD	Bacterial carbon demand	61 ± 20		65 ± 25
	f–*e*	% POC remineralization	10%		11%
150	$POCF_{150}$	NBST POC flux (Buessseler et al., 2007a)	68 ± 2		23 ± 2
	1–*e*	% POC remineralization	87%		94%

Carbon flux rates were assessed as described in the text. Values are mean ± standard error. The standard error of the mean reflects the sampling variability.

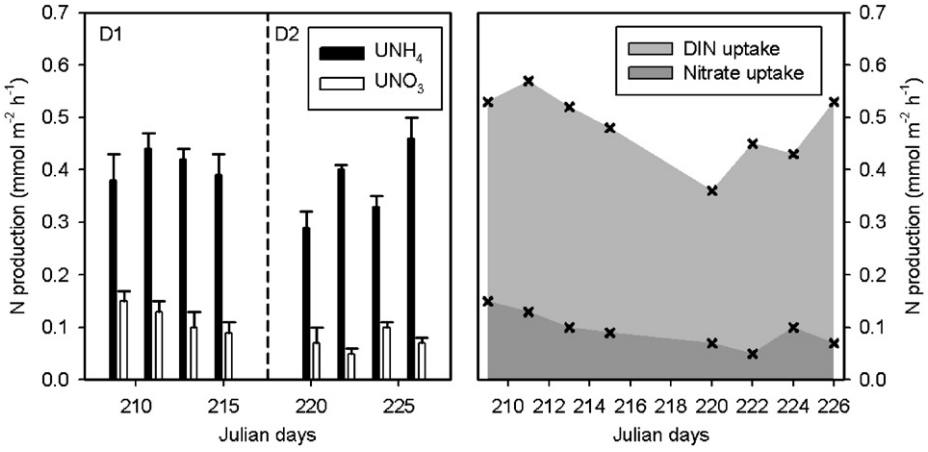

Fig. 7. Depth-integrated nitrogen based production (0–50 m) during the trap deployments (D1 and D2). The error bars represent the uncertainty on rate calculations (propagation of random errors, Section 2.8).

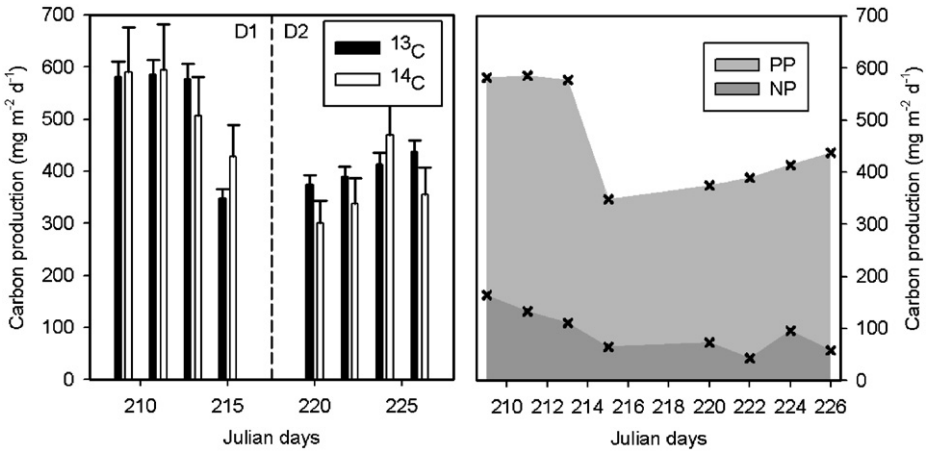

Fig. 8. Depth-integrated primary and new productions (0–50 m) during the trap deployments (D1 and D2). The error bars represent the uncertainty on rate calculations (propagation of random errors, section 2.8).

(the bacterial conversion of organic nitrogen back to ammonium) and direct zooplankton excretion or release. Accordingly, we estimated the bacterial contribution to ammonium production to be around 47–94%. The vertical profiles of ammonium assimilation (phytoplankton and bacterial uptake) and production (zooplankton and bacterial release) are shown in Fig. 11 with depth-integrated

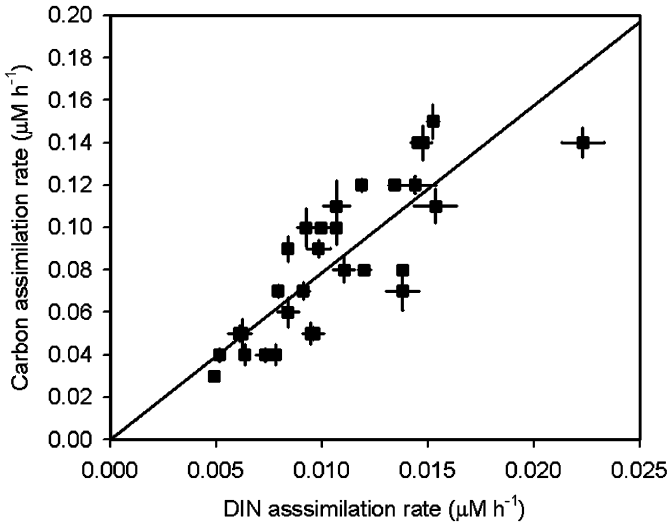

Fig. 9. Relation between carbon and nitrate assimilation rates. The error bars represent the uncertainty on rate calculations (propagation of random errors, Section 2.8). The slope UC/UDIN = 7.6 (SE = 1.0, $p<0.001$). SE: standard error. The p value is the probability that the slope does not differ from 0.

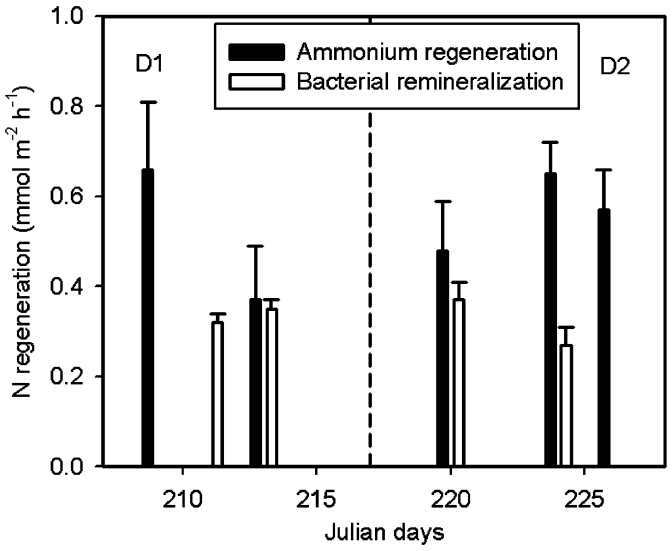

Fig. 10. Depth-integrated ammonium production and bacterial mineralization (0–50 m) during the trap deployments (D1 and D2). The error bars represent the uncertainty on rate calculations (propagation of random errors, Section 2.8).

values on the order of 0.39 and 0.57 mmol m^{-2} h^{-1}, respectively. This provides a net ammonium production rate of 0.18 mmol m^{-2} h^{-1}, which matches the trend for the build-up of ammonium stock observed in Fig. 4, i.e. 0.13 (SE = 0.02) mmol m^{-2} h^{-1}.

3.4. Carbon budget in the upper 150 m at K2

Since estimates of primary and new production have been made in the euphotic zone, and sinking flux of particulate organic carbon were collected at 150 m, it is possible to assess the balance between autotrophic and heterotrophic processes during our sampling period. During the trap deployment, K2 was characterized both by changes in primary, new and export production (Table 2). The data indicate that 17–23% of primary production is exportable to deeper layers (f ratio), but only 6–13% collected as a

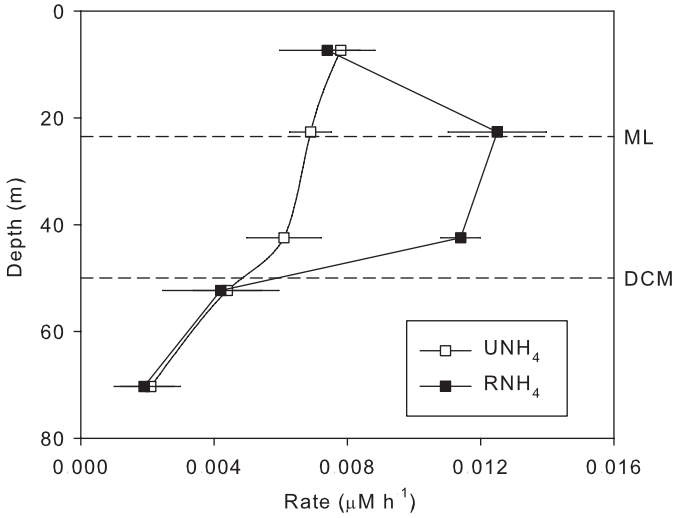

Fig. 11. Averaged profiles ($n = 5$) of ammonium assimilation and regeneration at K2. The error bars represent the sampling variability and are expressed as standard error of the mean.

sinking particle flux at 150 m (e ratio; Buesseler et al., 2007a). Hence, 77–85% of the carbon fixed by phytoplankton would be mineralized in the upper 50 m ($1-f$ ratio), while <11% would be within 50 and 150 m ($f-e$ ratios). Yet this information should carefully be considered since neither f and e ratios represent a fractional POC export assessed on a seasonal or steady state basis. The annual f (42%) and e ratios (29%) in the western subarctic gyre (Kawakami and Honda, 2007) were greater than those reported in this study. This is not too surprising since with an assemblage dominated by picoplankton (50–59%) there will be little sinking of biogenic material unless the cells aggregate, and we just passed over the new production peak. In contrast herewith, the difference in the percentage of the export ratio e is likely due to methodological issues. Kawakami and Honda (2007) estimated the POC flux from the surface layer using ^{234}Th as a tracer. At K2, these fluxes varied seasonally from 57 to 179 mg C m^{-2} d^{-1} and were much higher during summer than those measured here with NBSTs (Table 2). Using surface altimetry and ADCP data, likely particle source funnels for the 150 m NBST were up to 40 km west and 20–40 km north during D1 or 20–40 km south during D2 (Buesseler et al., 2008—this issue). Further comparisons among the VERTIGO traps, and between the VERTIGO results are discussed in companion papers (Buesseler et al., 2008; Lamborg et al., 2008; Trull et al., 2008). With a POC loss rate of 77 mg C m^{-2} d^{-1} in the upper 50 m (see Fig. 5), one can estimate the quantity of carbon available to meet the metabolic requirements of the heterotrophic community (HCD) with

$$\frac{dPOC}{dt} = NPP - HCD - NP \quad (8)$$

where NPP stands for net primary production and NP for new production, assumed to represent the exportable carbon flux out of the euphotic zone. Within this context, it should be stressed that our NP estimates (D1: 119 ± 42 and D2: 67 ± 23 mg C m^{-2} d^{-1}) are consistent with predicted POC export values of 66–166 (D1) and 23–43 (D2) mg C m^{-2} d^{-1} computed with a planktonic foodweb model (Boyd et al., 2008, this issue). In this model, two scenarios were selected to constrain the upper and lower bounds of the predicted export flux. The lower value corresponds to a fecally mediated flux where all NPP is transformed by a micro- and meso-zooplankton (copepod) dominated foodweb into fecal material, which exits the base of the euphotic zone. The upper value corresponds to an algal/fecal mediated flux in which all of

Table 3
Nitrogen budget at K2

Depth (m)	Symbol	Nitrogen flux rate (μmol m^{-2} h^{-1})	D1 31/07–06/08/05	D2 11/08–16/08/05
0–50	UDIN	DIN uptake	525 ± 18	443 ± 35
	UNH_4	Ammonium uptake	408 ± 14	370 ± 37
	UNO_3	Nitrate uptake	118 ± 14	73 ± 11
	RNH_4	Ammonium regeneration	570 ± 80	
	RNO_3	Nitrate regeneration	< MDL	
	dPN/dt	Rate of PN change (Fig. 5A)	−40 ± 6	
	HND	Available N for heterotrophic community Eq. (9)	447 ± 23	410 ± 37
	UNH_4/UDIN	%PN remineralization	78%	84%
0–150	dPN/dt	Rate of PN change	~0	
	UNO_3	Exportable N flux	118 ± 14	73 ± 11
	HND	Available N for heterotrophic community Eq. (9)	93 ± 14	64 ± 11
	(UNO_3–PNF_{150})/UDIN	%PN remineralization	17%	14%
150	PNF_{150}	NBST PN flux (Buesseler et al., 2007a)	25 ± 2	9 ± 1
	1–PN_F/UDIN	%PN remineralization	95%	98%

Nitrogen flux rates were assessed as described in the text. Values are mean ± standard error. The standard error of the mean reflects the sampling variability.

NPP by >20 μm cells exits the euphotic zone as intact cells, but all of the NPP by cells <20 μm is transformed by the pelagic foodweb.

Table 2 indicates that in the trophogenic zone, HCD is roughly equivalent to the primary production rate, and represents between 43% and 67% of the incoming new production flux in the subsurface layer (50–150 m). In the top 50 m, the median of the bacterioplankton carbon demand (the carbon required for respiration and growth) was estimated to be about 340 mg C m^{-2} d^{-1}, which is equivalent to >70% of the primary production. If we assume that bacteria and zooplankton graze only on phytoplankton, then the bacterial demand for carbon far outweighed the zooplankton demand for carbon fixed by photosynthesis within the euphotic zone. This is, however, a questionable assumption since the dissolved and particulate organic carbon utilized by bacteria is generated by a number of different processes including copepods grazing on microzooplankton and microzooplankton grazing on bacteria themselves. It follows that this assumption will probably maximize the demand of bacteria for phytoplankton production, and hence minimize the quantity available for micro- and meso-zooplankton grazing (carbon assimilated for use in respiration, growth, excretion, and reproduction). It should be noted that the feeding rate of the copepod community on the mixed-layer phytoplankton was estimated around 60–105 mg C m^{-2} d^{-1}, representing <20% of the primary production (Kobari et al., 2008, this issue). This suggests that microzooplankton could be both the main herbivores, and an important prey source for copepods in the euphotic zone (Boyd et al., this issue). Between 50 and 150 m the carbon requirement of bacteria decreased to 60 mg C m^{-2} d^{-1}, which is equivalent to the carbon available for the whole heterotrophic demand (Table 2). Dissolved organic carbon (DOC) is another important source that has not been addressed directly in the present analysis although it is involved in the HCD estimates, e.g. release of DOC during grazing. Moreover, not all of the exportable carbon estimated from new production is exported as a vertical POC flux; part may be exported out of the area by advective transport of either POC or DOC (Bronk et al., 1994). In the mesopelagic (below 150 m) the vertical supply of DOC from the euphotic zone could support a portion of the heterotrophic carbon demand, but not sufficiently (Steinberg et al., 2008). Instead, the mesopelagic carbon demand is probably sustained by the surface feeding of migrating zooplankton and their transport back to deeper layers, where they can excrete dissolved organic matter and release fecal pellets (Steinberg et al., 2008). This observation must be taken into account for the interpretation of data in Table 2 since it would bypass the shallow traps.

3.5. Nitrogen budget in the upper 150 m at K2

From the measured 150 m PN flux to the inorganic nitrogen production ratio, it can be stated that ~95–98% of nitrogen would be mineralized in the upper 150 m during D1 and D2, respectively (Table 3). Fig. 11 suggests that most of the shallow nitrogen mineralization occurred just above the DCM (20–40 m) where a net ammonium production was found. Nitrification rates being below detection, it is assumed that the nitrate utilization by phytoplankton was balanced by the supply of nitrate from below the euphotic zone (Table 3). As for C, the nitrogen metabolic requirement of the heterotrophic community (HND) was assessed with the following mass balance differential equation:

$$\frac{\mathrm{dPN}}{\mathrm{d}t} = \mathrm{UDIN} - \mathrm{HND} - \mathrm{UNO_3} \quad (9)$$

where UDIN stands for dissolved inorganic nitrogen-based production and UNO_3 for the nitrate uptake, i.e., assumed to be equivalent to the exportable N flux.

The results are very similar to those obtained for carbon in the upper 50 m, i.e., HND is roughly equivalent to the autotrophic nitrogen based production (Table 3). In the subsurface layer (50–150 m), HND represents more than 80% of the incoming vertical nitrogen flux, which possibly reflect the regeneration and use of nitrogenous labile compounds (ammonium and nitrite) immediately below the DCM as suggested in Fig. 3. Also, these results for extensive shallow N regeneration are supported by estimates of shallow PN remineralisation determined by Buesseler et al. (2008—this issue) by comparing the longer-term seasonal changes in upper ocean N stocks to the 150 m PN flux.

4. Conclusions and summary

During summer 2005, it is clearly apparent that C and N uptake in the euphotic zone were not sufficiently rapid to overcome grazing pressure and sinking losses. Biomass did not build-up, because of the small size of the phytoplankton population (0.2–2 μm), which provides 50–59% of the total production (Boyd et al., 2008—this issue), and which likely chose ammonium over nitrate as nitrogen substrate. High rates of new production were not attained as a result of both low specific nitrate uptake (0.025–0.010 d^{-1}) and low biomass (<60 and 350 mmol m^{-2} for PN and POC in the upper 50 m). According to our estimates, the available carbon and nitrogen for herbivores were roughly equivalent to primary production. Recycling within the water

column is the dominant process, and C–N assimilated by phytoplankton were rapidly regenerated and consumed by heterotrophs within or just below the euphotic zone (Table 2 and 3). As determined from SeaWIFS images (Honda and Watanabe, 2007), we just captured the end of a diatom bloom. The decrease in *f* ratio (28–17%) and new production followed the collapse of the bloom. The contribution of large diatom cells $>20\,\mu m$ to total production decreased from 30% to 19% between trap deployments (Boyd et al., 2008, this issue). Competition for ammonium, which can be induced by heterotrophic bacteria, could select for small cells and may force large diatoms to use nitrate. This implies that under Fe stress as observed here, ammonium uptake was preferred and new production progressively suppressed despite the surplus of nitrate. More controversy has arisen over the interpretation that new production represents an export flux of particles out of the euphotic zone (Eppley, 1989; Platt et al., 1992; Bronk et al., 1994; Yool et al., 2007) and NP could be better considered as "exportable" rather than an export flux. At K2, the ratio *e*/*f*, equivalent to the ratio of export (0–150 m) to new production (0–50 m) ranged from 0.34 to 0.57 within the range of most previous estimates in the North Pacific Ocean (Kawakami and Honda, 2007 and references therein). It suggests that 52–44 mg C m^{-2} d^{-1} of new production should be grazed and/or released as DOC between 50 and 150 m. These values are not unfounded regarding the metabolic carbon demand estimated for euphotic (Kobari et al., 2008, this issue) and mesopelagic (Steinberg et al., 2008) biota.

Acknowledgments

We acknowledge the skillful assistance of captain and crew of R/V *Revelle* during work at sea. This research was supported by the Research Foundation Flanders through Grant G.0021.04 and Vrije Universiteit Brussel via Grant GOA 22, as well as the US National Science Foundation programs in Chemical and Biological Oceanography. We also extend our thanks to the anonymous reviewers for their many fruitful comments.

References

Boyd, P.W., Gall, M.P., Silver, M., this issue. Quantifying the surface-subsurface biogeochemical coupling during the VERTIGO HOT and K2 experiments.

Bronk, D.A., Glibert, P.M., Ward, B.B., 1994. Nitrogen uptake, dissolved organic nitrogen release, and new production. Science 265, 1843–1846.

Buesseler, K.O., Benitez-Nelson, C.R., Moran, S.B., Burd, A., Charette, M., Cochran, J.K., Coppola, L., Fisher, N.S., Fowler, S.W., Gardner, W.D., Guo, L.D., Gustafsson, O., Lamborg, C., Masque, P., Miquel, J.C., Passow, U., Santschi, P.H., Savoye, N., Stewart, G., Trull, T., 2006. An assessment of particulate organic carbon to thorium-234 ratios in the ocean and their impact on the application of ^{234}Th as a POC flux proxy. Marine Chemistry 100, 213–233.

Buesseler, K.O., Lamborg, C.H., Boyd, P.W., Lam, P.J., Trull, T.W., Bidigare, R.R., Bishop, J.K.B., Casciotti, K.L., Dehairs, F., Elskens, M., Honda, M., Karl, D.M., Siegel, D., Silver, M.W., Steinberg, D.K., Valdes, J., Van Mooy, B., Wilson, S., 2007a. Revisiting carbon flux through the ocean's twilight zone. Science 316, 567–570.

Buesseler, K.O., Antia, A.N., Chen, M., Fowler, S.W., Gardner, W.D., Gustafsson, O., Harada, K., Michaels, A.F., Rutgers van der Loeff, M., Sarin, M., Steinberg, D.K., Trull, T., 2007b. An assessment of the use of sediment traps for estimating upper ocean particle fluxes. Marine Chemistry. Journal of Marine Research 65 (3), 345–416.

Buesseler, K.O., Trull, T.W., Steinberg, D.K., Silver, M.W., Siegel, D.A., Saitoh, S.-I., Lamborg, C.H., Lam, P.J., Karl, D.M., Jiao, N.Z., Honda, M.C., Elskens, M., Dehairs, F., Brown, S.L., Boyd, P.W., Bishop, J.K.B., Bidigare, R.R., 2008. VERTIGO (VERtical Transport In The Global Ocean): A study of particle sources and flux attenuation in the north pacific. Deep-Sea Research II, this issue [doi:10.1016/j.dsr2.2008.04.024].

Carlson, C.A., Ducklow, H.W., Sleeter, T.D., 1996. Stocks and dynamics of bacterioplankton in the northwestern Sargasso Sea. Deep Sea Research II 43, 491–515.

Currie, L.A., 1995. Nomenclature in evaluation of analytical methods including detection and quantification capabilities (IUPAC recommendations 1995). Pure and Applied Chemistry 67, 1699–1723.

D'Elia, C., 1983. Nitrogen determination in seawater. In: Carpenter, E.J., Capone, D.G. (Eds.), Nitrogen in the Marine Environment. Elsevier, New York, pp. 731–762.

de Brauwere, A., De Ridder, F., Elskens, M., Schoukens, J., Pintelon, R., Baeyens, W., 2005a. Refined parameter and uncertainty estimation when both variables are subject to error. Case study: estimation of Si consumption and regeneration rates in a marine environment. Journal of Marine Systems 55, 205–221.

de Brauwere, A., De Ridder, F., Pintelon, R., Elskens, M., Schoukens, J., Baeyens, W., 2005b. Model selection through a statistical analysis of the minimum of a weighted least squares cost function. Chemometrics and Intelligent Laboratory Systems 76, 163–173.

del Giorgio, P.A., Cole, J.J., 2000. Bacterial energetics and growth efficiency. In: Kirchman, D.L. (Ed.), Microbial Ecology of the Oceans. Wiley, pp. 289–325.

Ducklow, H., 2000. Bacterial production and biomass in the oceans. In: Kirchman, D.L. (Ed.), Microbial Ecology of the Oceans. Wiley, pp. 85–152.

Dugdale, R.C., Goering, J.J., 1967. Uptake of new and regenerated forms of nitrogen in primary productivity. Limnology and Oceanography 12, 196–206.

Dugdale, R.C., Wilkerson, F., 1992. Nutrient limitation of new production in the sea. In: Falkowski, P.G., Woodhead, A.D. (Eds.), Primary Productivity and Biogeochemical Cycles in the Sea. Plenum Press, New York and London, pp. 107–122.

Elskens, M., Penninckx, M., Vandeloise, R., Vander Donckt, E., 1988. Use of simplex technique and contour diagrams for the determination of the reaction rate constants between glutathione and thiram in the presence of NADPH. International Journal of Chemical Kinetics 20, 837–848.

Elskens, M., Baeyens, W., Cattaldo, T., Griffith, B., Dehairs, F., 2002. N-uptake conditions during the summer in the sub-Antarctic and polar frontal zones of the Australian sector of the southern ocean. Journal of Geophysical Research 107, 31–311.

Elskens, M., Baeyens, W., Brion, N., De Galan, S., Goeyens, L., de Brauwere, A., 2005. Reliability of N flux rates estimated from ^{15}N enrichment and dilution experiments in aquatic systems. Global Biogeochemical Cycles 19, GB4028.

Elskens, M., de Brauwere, A., Beucher, C., Corvaisier, R., Savoye, N., Tréguer, P., Baeyens, W., 2007. Statistical process control in assessing production and dissolution rates of biogenic silica in marine environments. Marine Chemistry.

Eppley, R.W., Peterson, B.J., 1979. Particulate organic matter flux and planktonic new production in the deep ocean. Nature 282, 677–680.

Eppley, R.W., 1989. New production: History, methods, problems. In: berger, W.H., Smetacek, V.S., Wefer, G. (Eds.), Productivity of the Ocean: Present and Past. Wiley, S. Bernhard, Dahlem Konferenzen, pp. 85–97.

Falkowski, P.G., 1997. Evolution of the nitrogen cycle and its influence on the biological sequestration of CO_2 in the ocean. Nature 387, 272–275.

Fuhrman, J.A., Azam, F., 1982. Thymidine incorporation as a measure of heterotrophic bacterioplankton production in marine surface waters: evaluation and field results. Marine Biology 66, 109–120.

Glibert, P.M., Capone, D.G., 1993. Mineralization and assimilation in aquatic, sediment and wetland systems. In: Knowles, R., Blackburn, T.H. (Eds.), Nitrogen Isotope Techniques. Elsevier, New York, pp. 243–272.

Hansen, H.P., Grasshoff, K., 1983. Automated chemical analysis. In: Grasshoff, K., Ehrhardt, M., Kremling, K. (Eds.), Methods of Sea Water Analysis, second ed. Verlag Chemie, Weinheim, Germany, pp. 368–376.

Harrison, W.G., 1983. Use of isotopes. In: Carpenter, E.J., Capone, D.G. (Eds.), Nitrogen in the Marine Environment. Academic Press, New York, London, pp. 763–807.

Harrison, W.G., Wood, L.J., 1988. Inorganic nitrogen uptake by marine picoplankton: evidence for size partitioning. Limnology and Oceanograpgy 33, 468–475.

Honda, M.C., 2003. Biological pump in the northwestern North Pacific. Journal of Oceanography 59, 671–684.

Honda, M.C., Watanabe, S., 2007. Utility of an automatic water sampler to observe seasonal variability in nutrients and DIC in the NW North Pacific. Journal of Oceanography 63, 349–362.

Honda, M.C., Kawakami, H., Sasaoka, K., Watanabe, S., Dickey, T., 2006. Quick transport of primary produced organic carbon to the ocean interior. Geophysical Research Letters 33.

Imaii, K., Nojiri, Y., Tsurushima, N., Saino, T., 2002. Time-series of seasonal variation of primary productivity at station KNOT (44°N, 155°E) in the sub-arctic western north pacific. Deep-Sea Research II 49, 5395–5408.

Kawakami, H., Honda, M.C., 2007. Time-series observation of POC fluxes estimated from ^{234}Th in the northwestern north pacific. Deep-Sea Research I 54, 1070–1090.

Kirchman, D.L., 1994. The uptake of inorganic nutrients by heterotrophic bacteria. Microbial Ecology 28, 255–271.

Kirchman, D.L., Keil, R.G., Wheeler, P.A., 1990. Carbon limitation of ammonium uptake by heterotrophic bacteria in the subarctic Pacific. Limnology and Oceanography 35, 1258–1266.

Kirchman, D.L., Keil, R.G., Simon, M., Welscmeyer, N.A., 1993. Biomass and production of heterotrophic bacterioplankton in the oceanic subarctic Pacific. Deep-Sea Research 40, 967–988.

Kobari, T., Steinberg, D.K., Ueda, A., Tsuda, A., Silver, M.W., Kitamura, M., 2008. Impacts of ontogenetically migrating copepods on downward carbon flux in the western subarctic Pacific Ocean. Deep-Sea Research II, this issue [doi:10.1016/j.dsr2.2008.04.016].

Koroleff, F., 1976. Determination of ammonia. In: Grasshoff, K. (Ed.), Methods of Seawater Analysis. Verlag Chemie, Weinheim, Germany, pp. 126–133.

Lamborg, C.H., Buesseler, K.O., Valdes, J., Bertrand, C.H., Manganini, S., Pike, S., Steinberg, D., Trull, T., Wilson, S., 2008. The flux of bio- and lithogenic material associated with sinking particles in the mesopelagic "twilight zone" of the

Northwest and North Central Pacific Ocean. Deep-Sea Research II, this issue [doi:10.1016/j.dsr2.2008.04.011].
Legendre, L., Gosselin, M., 1996. Estimation of N or C uptake rates by phytoplankton using ^{15}N or ^{13}C: revisiting the usual computation formulae. Journal of Plankton Research 19, 263–271.
Longhurst, A.R., Harrison, W.G., 1989. The biological pump—profiles of plankton production and consumption in the upper ocean. Progress in Oceanography 22, 47–123.
Maldonato, M.T., Price, N.M., 1996. Influence of N substrate on Fe requirements of marine centric diatoms. Marine Ecology Progress Series 141, 161–172.
Mandel, J., 1964. The Statistical Analysis of Experimental Data. Wiley, New York.
Nieuwenhuize, J., Maas, Y.E.M., Middelburg, J., 1994. Rapid analysis of organic carbon and nitrogen in particulate materials. Marine Chemistry 45, 217–224.
Orcutt, K.M., Lipschultz, F., Gundersen, K., Arimoto, R., Michaels, A.F., Knap, A.H., Gallon, J.R., 2001. A seasonal study of the significance of N-2 fixation by *Trichodesmium* spp. at the Bermuda Atlantic time-series Study (BATS) site. Deep-Sea Research II 48, 1583–1608.
Pace, M.L., Knauer, G.A., Karl, D.M., Martin, J.H., 1987. Primary production, new production and vertical flux in the Eastern Pacific. Nature 325, 803–804.
Platt, T., Jauhari, P., Sathyendranath, S., 1992. The importance of measurement of new production. In: Falkowski, P.G., Woodhead, A.D. (Eds.), Primary Productivity and Biogeochemical Cycles in the Sea. Plenum Press, New York and London, pp. 275–284.
Reuer, M.K., Barnett, B.A., Bender, M.L., Falkowski, P.G., Hendricks, M.B., 2007. New estimates of Southern Ocean biological production rates from O_2/Ar ratios and the triple isotope composition of O_2. Deep-Sea Research I 54, 951–974.
Sambrotto, R.N., Mace, B.J., 2000. Coupling of biological and physical regimes across the Antarctic Polar Front as reflected by nitrogen production and recycling. Deep-Sea Research II 47 (15–16), 3339–3367.
Suter, G.W., 2007. Variability, uncertainty and probability. In: Ecological Risk Assessment. CRC Press, Boca Raton, London, New York, pp. 69–94.
Steinberg, D.K., Van Mooy, B.A.S., Buesseler, K.O., Boyd, P.W., Kobari, T., Karl, D.M., 2008. Microbial vs. zooplankton control of sinking particle flux in the ocean's twilight zone. Limnology and Oceanography 53 (4).
Trull, T.W., Bray, S., Buesseler, K.O., Lamborg, C.H., Manganini, S., Moy, C., Valdes, J., 2008. In-situ measurement of mesopelagic particle sinking rates and the control of carbon transfer to the ocean interio during the Vertical Flux in the Global Ocean (VERTIGO) voyages in the North Pacific. Deep-Sea Research II, this issue [doi:10.1016/j.dsr2.2008.04.021].
Wong, C.S., Waser, N.A.D., Nojiri, Y., Whitney, F.A., Page, J.S., Zeng, J., 2002. Seasonal cycles of nutrients and dissolved inorganic carbon at high and mid latitudes in the North Pacific Ocean during the Skaugran cruises: determination of new production and nutrient uptake ratios. Deep-Sea Reearch II 49, 5317–5338.
Yool, A., Martin, A.P., Fernandez, C., Clark, D.R., 2007. The significance of nitrification for oceanic new production. Nature 447, 999–1002.
Zhang, Y., Jiao, N.Z., Hong, N., 2008. Comparative studies on picoplankton biomass and community structure in different provinces from subarctic to subtropical oceans. Deep-Sea Research II, this issue [doi:10.1016/j.dsr2.2008.04.014].